



Minerva Access is the Institutional Repository of The University of Melbourne

**Author/s:**

Bribiesca-Contreras, G;Verbruggen, H;Hugall, AF;O'Hara, TD

**Title:**

Global biogeographic structuring of tropical shallow-water brittle stars

**Date:**

2019-07-01

**Citation:**

Bribiesca-Contreras, G., Verbruggen, H., Hugall, A. F. & O'Hara, T. D. (2019). Global biogeographic structuring of tropical shallow-water brittle stars. *Journal of Biogeography*, 46 (7), pp.1287-1299. <https://doi.org/10.1111/jbi.13620>.

**Persistent Link:**

<https://hdl.handle.net/11343/285955>

1

2 DR. GUADALUPE BRIBIESCA-CONTRERAS (Orcid ID : 0000-0001-8163-8724)

3

4

5 Article type : Research Paper

6

7

8 **Global biogeographic structuring of tropical shallow-water brittle stars**

9

10 **Running title:** Phylodiversity of tropical brittle stars

11

12 Guadalupe Bribiesca-Contreras\*<sup>1,2</sup>, Heroen Verbruggen<sup>2</sup>, Andrew F. Hugall<sup>1</sup>, Timothy D. O'Hara<sup>1</sup>13 <sup>1</sup> Museums Victoria, GPO Box 666, Melbourne, VIC 3001, Australia14 <sup>2</sup> School of Biosciences, The University of Melbourne, Melbourne, Victoria 3010, Australia

15 \* Corresponding author: l.bribiesca-contreras@nhm.ac.uk

16

17 **Acknowledgments**

18 T.O.H., A.F.H. and G.B.C. (partially) received support from the Marine Biodiversity Hub, funded  
19 through the National Environmental Research Program (NERP), and administered through the  
20 Australian Government's Department of the Environment. G.B.C. received support from the  
21 University of Melbourne (MIRS/MIFRS) and the Albert Shimmins Fund. H.V. was supported by the  
22 Australian Research Council (FT110100585).

23

24 **ABSTRACT**

This is the author manuscript accepted for publication and has undergone full peer review but has not been through the copyediting, typesetting, pagination and proofreading process, which may lead to differences between this version and the [Version of Record](#). Please cite this article as [doi: 10.1111/jbi.13620](https://doi.org/10.1111/jbi.13620)

This article is protected by copyright. All rights reserved

25 Aim: Biogeographic barriers emerged in the tropical oceans as continental masses moved with plate  
26 tectonics, and as the tropics contracted to lower latitudes from the late Eocene. These barriers have  
27 shaped tropical marine biodiversity. We characterise large-scale diversity patterns for tropical brittle  
28 stars and investigate the effect of biogeographic barriers on these in space and time.

29 Location: Shallow-water (<200 m) tropical oceans.

30 Taxon: Tropical shallow-water brittle stars.

31 Methods: We integrate phylogenetic and biogeographic modelling to test and quantify the  
32 biogeographic structuring across the major ocean basins for five families of brittle stars. These are  
33 well sampled in our phylogenies (173 species) and represent an important component of the brittle-  
34 star fauna of tropical shallow waters. We define major bioregions based on patterns of compositional  
35 and phylogenetic beta diversity.

36 Results: We find congruence between patterns of shared ancestry of regions and inferred  
37 biogeographic histories. Biogeographic reconstructions show that faunal patterns reflect the  
38 emergence of biogeographic barriers in the tropical world, with evidence of vicariant events driven by  
39 the opening of the Atlantic Ocean, the narrowing of the Tethyan Seaway and the rise of the Isthmus of  
40 Panama.

41 Main conclusions: Biogeographic barriers almost completely isolated regional faunas. However,  
42 divergence age estimates predate the onset of the different barriers, suggesting that changes associated  
43 with the gradual emergence of the barriers had a strong effect on the evolutionary history of tropical  
44 shallow-water brittle stars. Limited, very recent, bi-directional dispersal was detected across the East  
45 Pacific Barrier, which is otherwise an important barrier for dispersal of brittle stars.

46

47 **Keywords:** Phylodiversity, tropical realm, Ophiuroidea, biogeographic barriers, plate tectonics,  
48 shallow-waters, dispersal

49

50 INTRODUCTION

51 In the tropical oceans, major biogeographic barriers have greatly influenced the diversification of  
52 several marine taxa, acting as drivers of speciation (e.g. Floeter et al., 2008; Cowman & Bellwood,  
53 2013). The tropical marine region has been restricted to low latitudes since the late Eocene-early  
54 Oligocene, with the initiation of the Antarctic Circumpolar Current (Kamp, Waghorn & Nelson,  
55 1990), and is currently considered to be divided into three major realms (Cowman & Bellwood,

56 2013): Indo-West Pacific (IWP), Atlantic (A; including Mediterranean Sea) and East Pacific (EP).  
57 Barriers to dispersal of marine fauna between these realms have emerged at different points  
58 throughout the geological history of the planet and have shaped the current distribution and diversity  
59 patterns of tropical shelf (<200 m depth) taxa (Cowman & Bellwood, 2013). The oldest of these, the  
60 opening of the Atlantic Ocean (*ca.* 110–65 million years ago [Ma]), separated the East Pacific and  
61 West Atlantic from the East Atlantic, Mediterranean Sea and Indo-Pacific (Greiner & Neugebauer,  
62 2013). The East Pacific Barrier (EPB), considered a permeable barrier of *ca.* 5000 km of deep water,  
63 has been acting throughout the past 65 Myr, separating the Indo-West Pacific from the East Pacific  
64 (Grigg & Hey, 1992). Dispersal between the tropical Atlantic and Indo-West Pacific oceans became  
65 progressively restricted by the closure of the Tethys Sea. The final closure, the Terminal Tethyan  
66 Event (TTE) when Africa collided with Arabia, occurred 18–12 Ma (Adams, Gentry & Whybrow,  
67 1983). The most recent barrier was the Isthmus of Panama (IoP), which progressively separated the  
68 tropical Atlantic from the East Pacific starting 15 Ma with final closure *ca.* 3 Ma (Lessios, 2008).

69 Brittle stars, a group of widespread benthic invertebrates (class Ophiuroidea), have been the target of  
70 recent studies addressing macroevolutionary processes, as an extensive phylogenomic dataset is  
71 available (Hugall, O'Hara, Hunjan, Nilsen & Moussalli, 2016; Bribiesca-Contreras, Verbruggen,  
72 Hugall & O'Hara, 2017; O'Hara et al., 2018). Most higher taxonomic ranks, down to genus, are widely  
73 distributed longitudinally (Stöhr, O'Hara & Thuy, 2012), with regional differences occurring only at  
74 species level (O'Hara, Hugall, Thuy, Stöhr & Martynov, 2017). Both shelf (<200 m) and upper-slope  
75 (200–2,000 m) depths show a negative latitudinal diversity gradient (O'Hara, Rowden & Bax, 2011;  
76 Stöhr et al., 2012). Diversity peaks have been identified in the Indo-West Pacific and western Atlantic  
77 Ocean (Woolley et al., 2016). Secondary peaks, such as the North Pacific, South Pacific and the  
78 Indian Ocean, rim the diverse Indo-West Pacific (Stöhr et al., 2012).

79 Improved phylogenies based on extensive genomic datasets are providing a better understanding of  
80 biodiversity patterns and its underlying processes. Patterns of diversity accounting for phylogenetic  
81 relationships, such as phylogenetic diversity metrics (PD; Faith, 1992), provide insight into the shared  
82 ancestry of regional faunas. Probabilistic models of geographic range evolution can identify processes  
83 generating spatio-temporal patterns (vicariance and dispersal; e.g. Ree, Moore, Webb & Donoghue,  
84 2005). However, different methods assume that processes shape geographic ranges in various ways,  
85 thus affecting the conclusions on biogeographic histories. For instance, some methods do not allow  
86 the inheritance of the full ancestral range (DIVA, dispersal-vicariance analysis; Ronquist, 1997),  
87 potentially overestimating vicariance (Buerki et al., 2011) in comparison with methods that allow a  
88 widespread range to be inherited (DEC, dispersal-extinction-cladogenesis ; Ree et al., 2005; Ree &  
89 Smith, 2008). Therefore, biogeographic models should be chosen based on prior knowledge on  
90 processes shaping distributional patterns. As suitable data is frequently lacking for many taxa,  
91 statistical model comparison has been utilised to determine which model best fits both the

92 phylogenetic and biogeographic data (Matzke, 2013), and model-averaging has also been used to  
93 account for model uncertainty (Araujo & New, 2007; Grueber, Nakagawa, Laws & Jamieson, 2011)  
94 and the complexity of real world biogeography.

95 The goal of this study is to characterise large-scale diversity patterns for brittle stars, focusing on the  
96 effect of biogeographic barriers on the diversity patterns of tropical lineages in space and time. Our  
97 approach consists of defining regions of evolutionary significance (RES) based on patterns of  
98 turnover of species and of phylogenetic diversity between biogeographic provinces, followed by  
99 estimation of ancestral ranges accounting for different scenarios. We use a multi model biogeographic  
100 inference approach in a time-calibrated phylogenetic context in order to investigate concordant  
101 patterns of diversification associated with biogeographic barriers in the tropical oceans.

102

## 103 **MATERIALS AND METHODS**

### 104 **Distributional records**

105 We focus on five families of brittle stars: Ophiocomidae Ljungman, 1867, Ophiolepididae Ljungman,  
106 1867, Ophionereididae Ljungman, 1867, Ophiotrichidae Ljungman, 1867, and Ophiodermatidae  
107 Ljungman, 1867. These families are an important component of the brittle star fauna of tropical, shelf  
108 habitats (<200 m), with most of their species being restricted to this biome (54 to 96 percent; Table 1,  
109 Fig. 1a, see also O'Hara et al. (2017)). Species distributional data was extracted from a global  
110 distributional dataset (Woolley et al., 2016).

111

### 112 **Phylogenetic inference and divergence dating**

113 Dated phylogenetic trees for the five families were estimated from a common phylogenomic super-  
114 matrix of 781 species comprising 1,462 exons (in 416 genes) and mitochondrial cytochrome oxidase  
115 subunit I gene (COI), amounting to a total length of 267k sites, which has been used in several  
116 previous studies (Bribiesca-Contreras et al., 2017; O'Hara et al., 2017; O'Hara, Hugall, Woolley,  
117 Bribiesca-Contreras & Bax, 2019). Bayesian relaxed-clock analyses of family-taxa subsets of this  
118 phylogenomic super-matrix were performed using BEAST v2.4 (Bouckaert et al., 2014). These  
119 analyses used sequence model, calibrations, and starting trees determined from those previous studies  
120 (see Supplementary Information for details).

121 Two independent runs were conducted for each of the five families and convergence assessed by  
122 congruence between individual run consensus trees and posterior ESS (>150) of combined runs  
123 (BEAST v2.4, TREEANNOTATOR, and TRACER v1.5; see Supplementary files 1–10). Maximum clade

124 credibility consensus trees (with median node heights) were then derived from the combined posterior  
125 samples (Figs S3–S7). Finally, sets of one hundred posterior samples per family were randomly  
126 selected to represent phylogenetic variation for biogeographic analyses (Supplementary Files 11–15).

127

## 128 **Regions of evolutionary significance**

129 Many different marine bio-regionalisation schemes have been proposed based on animal and algal  
130 distributions or environmental surrogates (e.g. Spalding et al., 2007; Costello et al., 2017). In the  
131 absence of an agreed scheme, we have derived our own regions of evolutionary significance (RES)  
132 based on species and phylogenetic turnover (beta diversity) metrics of our sampled organisms.  
133 Distribution records were categorised into local marine provinces from Spalding et al. (2007). The 39  
134 provinces, for which we had relevant distributional records, included tropical and some neighbouring  
135 warm-temperate provinces (Table S1 and Fig. S2).

136 We estimated the Pearson's product-moment correlation coefficient (PPMCC, 'stats' R package; R  
137 Core Team, 2017) between species richness by regions, as obtained from the distributional dataset,  
138 and the sampled-species richness to assess whether species richness patterns from DNA-sampled taxa  
139 (Fig. S2) correlated with the distributional dataset. Deep-sea and non-tropical species, as well as  
140 duplicates of tropical shelf species were pruned from each chronogram ('ape' R package; Paradis,  
141 Claude & Strimmer, 2004). In most cases, deep-sea or non-tropical taxa represented monophyletic  
142 clades which did not contribute to the biogeographical processes being examined here (Table 1; Figs.  
143 S3–S7 for details on pruned taxa). Since the distribution of species within the *Ophiothrix fragilis*  
144 (Abildgaard in O.F. Müller, 1789) complex along the West African coast is not well understood, we  
145 retained only a single sequence to represent this monophyletic complex. Although *Ophiothela*  
146 *mirabilis* Verrill, 1867 has been recorded for both the Eastern Pacific and Atlantic oceans, we  
147 assessed it to be an Eastern Pacific endemic as it is considered a recent introduction into the Atlantic  
148 Ocean (Mantelatto et al., 2016).

149 Species, or Compositional, Beta Diversity (CBD) was quantified for all pairs of provinces using  
150 Sørensen (Sor) dissimilarity index from a presence/absence matrix obtained from species occurrence  
151 data ('betapart' R package; Baselga & Orme, 2012). This index was decomposed into turnover (Sor<sub>turn</sub>,  
152 replacement of species; equivalent to Simpsons dissimilarity index) and nestedness (Sor<sub>ne</sub>, where  
153 assemblages with few species are subsets of richer sites) components (Baselga, 2010; Baselga &  
154 Orme, 2012). Phylogenetic Beta Diversity (PBD), which accounts for the phylogenetic relatedness  
155 between species, was also quantified for all pairs of provinces using a modified Sørensen index, pSor  
156 (Leprieur et al., 2012); and its turnover (pSor<sub>turn</sub>) and nestedness (pSor<sub>ne</sub>) components.

157 Dissimilarity matrices, for each component of both CBD and PBD, were estimated independently for  
158 each family, as they are dispersed throughout the phylogeny of the class Ophiuroidea (Fig. S1)  
159 (O'Hara et al., 2017). This also avoided including ancient (>100 Ma) inter-familial relationships that  
160 predated the biogeographic processes being investigated. A single dissimilarity matrix was then  
161 generated by averaging the dissimilarity matrices of each of the five families. This increased the  
162 number of species per province, increasing the power of inference, and subsequent analyses used this  
163 averaged dissimilarity matrix.

164 We used the turnover fraction of both metrics ( $Sor_{turn}$  and  $pSor_{turn}$ ) as the basis for grouping provinces  
165 into larger RES, performing both hierarchical clustering and nonmetric multidimensional scaling  
166 (NMDS). Optimal number of clusters was estimated using the Kelley-Gardner-Sutcliffe penalty  
167 function (KGS; see Supplementary Information). Significance of PBD between pairs of RES was  
168 assessed by testing if observed values of PBD re explained by taxonomic composition (CBD) alone.  
169 This was done by comparing each fraction of the phylogenetic beta diversity metric against a null  
170 model based on keeping the species diversity constant but resampling the underlying phylogenetic  
171 diversity by randomising the tree tip labels 1,000 times. Standardised effect size (SES) was calculated  
172 for each component as in Leprieur et al. (2012), which indicates if regions are less ( $\leq -1.96$ ) or more  
173 ( $\geq 1.96$ ) phylogenetically similar than expected just from their compositional similarity.

174

## 175 **Biogeographic analyses**

176 Historical biogeographic reconstructions were performed under a biogeographic event-based model  
177 that considers both vicariance and dispersal as processes, DEC (Ree et al., 2005). The Bayesian  
178 implementation of this model (Landis, Matzke, Moore & Huelsenbeck, 2013), in REVBAYES (Höhna  
179 et al., 2016), has been used for testing different biogeographic scenarios (Lavor, Calvente, Versieux &  
180 Sanmartin, 2018). We used species distributions categorised into the three RES, as delimited from  
181 beta diversity patterns (A, Atlantic; EP, East Pacific; and IWP, Indo-West Pacific). Simple DEC  
182 analyses considered allopatric ('a') and subset sympatric ('s') events, but full sympatry ('f') and jump  
183 dispersal ('j') can be included. We did not include jump dispersal due to concerns raised by Ree and  
184 Sanmartín (2018). Simple DEC ('s' and 'a') and DEC models with full sympatry ('s', 'a', and 'f')  
185 were compared using the ratio of marginal likelihoods with Bayes Factor (Thode, Sanmartin &  
186 Lohmann, 2019). Biogeographic inference was performed under both models using the consensus  
187 BEAST tree, for each family. Six independent runs of MCMC were performed, sampling every 10 in  
188 10,000 samples, following the REVBAYES tutorial (Michael Landis,  
189 <http://revbayes.github.io/tutorials.html>). Marginal likelihood estimators (MLE; log-likelihoods) were  
190 estimated both via 50 steps of Stepping Stone (SS) and Path Sampling (PS) during the MCMC and ln-  
191 Bayes factor estimated as  $\ln BF = MLE_{model1} - MLE_{model2}$  (Kass & Raftery, 1995).

192 Based on lnBF (Table S4), with values <1 (Ophionereididae) supporting the simple model over the  
193 more complex DEC model and near zero (Ophiotrichidae, Ophiolpididae, Ophiocomidae, and  
194 Ophiodermatidae) indicating no preference for either, biogeographic inferences were performed using  
195 simple DEC. To account for both phylogenetic uncertainty and uncertainty in age estimation, analyses  
196 were performed using the set of 100 BEAST trees for each family. A single MCMC chain was run  
197 sampling 10/10,000 and discarding 25% as burnin.

198 Ancestral states were summarised across the sample of 100 BEAST trees, for each family, onto the  
199 consensus tree. Effective Sample Sizes (ESS) were estimated to check for convergence of each  
200 MCMC run, and the run discarded if ESS<200 (none for Ophiocomidae, Ophiotrichidae and  
201 Ophionereididae, one for Ophiolpididae, and four for Ophiodermatidae). Only nodes defining clades  
202 from the consensus tree were considered in each posterior sample tree, which were identified based on  
203 their descendants. Ancestral states for each node, on each tree, were recovered from the end state  
204 column corresponding to each node from the ancestral state trace files generated in REVBAYES  
205 (Höhna et al., 2016).

206 As a comparison, biogeographic histories were also inferred under DEC and DIVA, implemented in  
207 'BioGeoBEARS' (Matzke, 2013) R package using a variety of constraints and parameters (see  
208 Supplementary), and performing model-averaging based on model weight (wAICc, Table S5).

209

## 210 **Faunal splits**

211 In order to investigate the potential effect of the established physical biogeographic barriers  
212 considered in this study, divergence times across specific barriers were compared within and between  
213 families to look for concordant patterns of lineage splitting across regions. We also recovered  
214 transitions at cladogenesis and estimated age for each node, for each BEAST posterior tree sample, as  
215 outlined previously. Transitions for each node were recovered from the start state columns, in the  
216 ancestral state tree trace files, corresponding to the direct descendants of each node. These transitions  
217 represent different speciation modes (e.g. sympatry or allopatry), and were summarised by node (with  
218 values from 0 to 1). Faunal splits were only considered from allopatric events where both daughter  
219 lineages were inferred to occur in different regions, therefore only including three transitions (A/EP,  
220 A/IWP, EP/IWP). The temporal distribution of faunal splits was plotted to show both uncertainty in  
221 age estimation and phylogenetic uncertainty in estimation of biogeographic histories. Thus, all  
222 transitions recovered from the ancestral state files were plotted ('ggbeeswarm' R package; Clarke &  
223 Sherrill-Mix, 2017) to show the fully integrated global biogeographic posterior temporal distribution  
224 of faunal splits across the three RES. As suggested by Crisp, Trewick and Cook (2011), vicariance

225 was rejected for faunal splits if the age range (95% HPD) estimates from the consensus BEAST tree  
226 did not overlap with the period associated with the emergence of the relevant biogeographic barrier.

227

## 228 RESULTS

### 229 Patterns of tropical beta diversity

230 Species richness for tropical brittle star peaked in provinces in the Central Indo-Pacific (Fig. 1a), with  
231 up to 90 species. The peripheral Indo-Pacific provinces, as well as Eastern Atlantic and Eastern  
232 Pacific provinces showed lower taxonomic diversity. The pattern of sampled-species richness by  
233 province (Table S1 and Fig. S2) was highly correlated with that for all species in the distributional  
234 dataset (Fig. 1a, PPMCC = 0.984,  $p\text{-val} < 2.2e-16$ ).

235 Three optimal clusters from the hierarchical clustering of CBD index  $Sor_{turn}$  (Fig. 1b and Fig. S8)  
236 were recovered, that could be designated as RES: 1) East Pacific (EP, yellow), 2) Atlantic (A, blue)  
237 and 3) Indo-West Pacific (IWP, red). The warm temperate African provinces of Agulhas and  
238 Benguela (Fig. 1d) were compositionally more similar to the Indo-West Pacific and Atlantic,  
239 respectively. Within-RES provinces, species turnover was low (Table S2). Alternatively, five optimal  
240 clusters were suggested from hierarchical clustering based on the PBD index  $pSor_{turn}$  (Fig. 1c),  
241 including two new clusters in addition to the three previously identified: 1) Benguela and 2) a cluster  
242 of three peripheral Indo-West Pacific provinces (Hawaii, Easter Island and Southern Polynesia).  
243 However, both these clusters were characterised by low species richness and some old endemic  
244 species (Table S1). The 3D nonmetric multidimensional scaling (NMDS) ordination of provinces  
245 based on  $pSor_{turn}$  values recovered Benguela as a transitional or an overlap region between the  
246 Atlantic+East Pacific and Indo-West Pacific provinces, while the three peripheral Indo-West Pacific  
247 provinces were grouped with other IWP provinces (Figs. 1a, d, S2, and S8). In addition, the few  
248 species distributed across both Atlantic and Indo-West Pacific mainly overlapped in Benguela and  
249 Agulhas (Fig. 1c). Therefore, these two additional clusters were considered unsuitable as separate  
250 regions in our selected macro-evolutionary analyses and we based subsequent biogeographic analyses  
251 on the dominant three major RES.

252 Within-RES provinces, phylogenetic beta diversity was mostly explained by nestedness (Table S2).  
253 No other subregional patterns of phylogenetic turnover were recovered within the Indo-West Pacific  
254 (e.g. separation of eastern African provinces). Within the Atlantic, provinces between East and West  
255 coasts appeared to be more phylogenetically dissimilar (median  $pSor_{turn}$ : 0.3, Table S3, Figs. 1d and  
256 S8) than between provinces within coasts (median  $pSor_{turn}$  west: 0.07; east excluding Benguela: 0.0;  
257 east including Benguela: 0.15). Between RES, the highest phylogenetic separation occurred between

258 the Indo-West Pacific and both the Atlantic and East Pacific RES ( $SES \geq 1.96$ ; Table 2, Fig. S8). On  
259 the contrary, the East Pacific and Atlantic were recovered as being phylogenetically similar despite  
260 their dissimilarity in compositional (species-level) assemblages ( $SES \leq -1.96$ ; Table 2).

261

## 262 **Biogeographic histories and regional faunal splits**

### 263 *Biogeographic histories*

264 The frequency of EP/IWP faunal splits peaked during the Pliocene/Pleistocene (A, Fig. 2), long after  
265 the establishment of the East Pacific Barrier (65 Ma). In the case of A/IWP faunal splits, four  
266 frequency peaks were observed (B–E). Three of these predated the TTE (B–D), with one coinciding  
267 with the time associated to the opening of the Atlantic Ocean (B) and two during the narrowing of the  
268 Tethyan Seaway (C–D). Most transitions were recovered within the narrowing of the Tethyan Seaway  
269 (C–D). Additionally, A/IWP faunal splits also peaked after the TTE, during the Late Miocene (E).  
270 Splits between East Pacific and Atlantic faunas peaked during the late Miocene (F), after the land  
271 bridge started to form (from mid Miocene) but before the complete emergence of the Isthmus of  
272 Panama in the Pliocene (~2.8 Ma), with some coinciding with the final emergence (G).

273

### 274 *Concordant patterns of regional transitions*

275 Faunal splits (allopatric events) were recovered for 29 nodes (Fig. 3). As a result of higher uncertainty  
276 in the ancestral range estimation for older nodes, mostly associated with A/IWP splits (Fig. 2), older  
277 faunal splits tended to have lower frequencies than recent nodes. In comparison, most A/EP faunal  
278 splits were recovered with higher frequencies.

279 Concordant patterns of faunal splits were observed across the five families (Fig. 3, S9a), which were  
280 also temporally concordant with the emergence of biogeographic barriers. These results were also  
281 concordant with biogeographic inferences performed in BioGeoBEARS (Fig. S9), where the preferred  
282 biogeographic model for each of the five families included dispersal constraint between RES after the  
283 emergence of the relevant biogeographic barriers (Table S5). Faunal splits between the Atlantic and  
284 Indo-West Pacific were estimated very early in the history of the families Ophiidermatidae (Fig. S9a)  
285 and Ophiotrichidae, in the former, during the time associated with the opening of the Atlantic Ocean.  
286 Across all families, half of the nodes (6/12) with A/IWP splits were concordant with the narrowing of  
287 the Tethyan Seaway, but pre-dated the TTE. A/IWP splits after the closure of the Tethyan Seaway  
288 were only recovered for a single node in the family Ophiocomidae (see also peak E in Fig. 3),  
289 associated with the genus *Ophiocomella* A.H. Clark, 1939. The fissiparous *Ophiocomella* species  
290 complex was longitudinally widespread in all three RES, but direction of dispersal is unclear as node

291 states for this species complex were not decisive in our analyses (Figs. 3, S10). In all families,  
292 Atlantic+East Pacific lineages were estimated to have diverged from Indo-West Pacific lineages. Only  
293 a few species within these clades are also distributed in the Indo-West Pacific, and only one restricted  
294 to the IWP (*Ophiothrix echinotecta* Müller & Troschel, 1840), distributed in the east African coast. In  
295 Ophiidermatidae, Ophiotrichidae, and Ophionereididae, the Atlantic+East Pacific species formed  
296 monophyletic clades, whereas in Ophiocomidae and Ophiolepididae, at least two divergence events  
297 were recovered.

298 Splits between the Atlantic and Indo-West Pacific were followed in time by multiple splits between  
299 the Atlantic and East-Pacific lineages, all except one occurring in a narrow time range corresponding  
300 to the emergence of the Isthmus of Panama (15–2.8 Ma). East-Pacific lineages, mostly represented by  
301 a single species, were recovered nested within Atlantic clades in all families. These faunal splits were  
302 estimated to occur 13 times, with at least two events recovered in each family (Table 3, Fig. 3).

303 Faunal splits between the East and Indo-West Pacific Oceans were only recovered with high  
304 frequencies for the families Ophiocomidae and Ophiotrichidae (Table 3, Fig. 3). However, these were  
305 inferred to occur very recently (Pliocene/Pleistocene). Since the EPB has been in place since the  
306 Paleocene, we interpret these as dispersal events across the barrier. An eastward dispersal was  
307 recovered for *Ophiocoma erinaceus* Müller & Troschel, 1842 (Ophiocomidae; Fig. S10). Although  
308 the dispersals of *Ophiothela mirabilis* Verrill, 1867 (Ophiotrichidae; Fig. S14) and *Ophiocomella*  
309 *sexradia* (Duncan, 1887) (Ophiocomidae; Fig. S10) were inferred to occur eastward and westward,  
310 respectively, there was no certainty in the direction of these recent dispersals. EP/IWP faunal splits  
311 were also recovered with low frequency for Ophionereididae during the Paleocene–Eocene (Figs. S9a,  
312 S13).

313

## 314 **Discussion**

315 Biogeographic studies have transitioned from describing patterns to inferring processes that shape  
316 spatio-temporal patterns (Sanmartín, 2007). Here, we reassessed diversity patterns in tropical shelf  
317 brittle stars, and reconstructed their biogeographic history to investigate the effect of the emergence of  
318 biogeographic barriers in their evolution. To improve biogeographic inferences, model selection was  
319 performed based on Bayes factor and phylogenetic uncertainty and uncertainty in divergence ages  
320 were taken into account. Additionally, the regions used for our global-scale analysis were defined  
321 based on patterns of beta diversity, as areas should be relevant to the hypotheses being tested (Ree &  
322 Sanmartín, 2009).

323

325 Both phylodiversity and model-based biogeographical approaches revealed a clear picture of the role  
326 of Earth history in shaping tropical brittle star diversity. Patterns of species and phylogenetic turnover  
327 (Fig. 1) across biogeographic provinces (Spalding et al., 2007) recovered three main regions, the  
328 Atlantic, East Pacific and Indo-West Pacific, which we used as RES. We also recovered strong  
329 patterns of phylogenetic regionalisation, with large clades being endemic to different RES. The  
330 Atlantic and East Pacific have a long history of shared ancestry and independent evolution from the  
331 Indo-West Pacific (Tables 2 and S2), suggesting a more recent isolation.

332 In reef fishes, conspicuous patterns of phylogenetic diversity were found within the Indo-West Pacific  
333 and the Atlantic Oceans (Cowman, Parravicini, Kulbicki & Floeter, 2017). For these taxa, the African  
334 coast and the Red Sea diversity differed from the rest of the Indo-West Pacific (Cowman et al., 2017).  
335 In other groups, diversity patterns differed between the West Indian Ocean and the West Pacific (e.g.  
336 Lessios, Kessing & Pearse, 2001), while we recovered no clear patterns within the Indo-West Pacific  
337 RES across the five families of brittle stars.

338 Differences in tropical reef fish diversity patterns were also found between the east and west Atlantic  
339 coasts (Cowman et al., 2017), where the mid-Atlantic represents a filter for dispersal with only few  
340 species dispersing through this wide stretch of water, mostly eastwards (Floeter et al., 2008). In brittle  
341 stars, we found Atlantic provinces to be more phylogenetically dissimilar between than within coasts,  
342 concordant with the patterns described for tropical reef fishes (Cowman et al., 2017). Most Atlantic  
343 brittle stars included in this study are restricted to either the east or west coast, with many more  
344 species occurring in the West. The lower diversity of the East Atlantic could be attributed to less  
345 extensive survey effort in the East, to restricted dispersal across the basin (Floeter et al., 2008) or to  
346 the lack of extensive coral reefs on the west African coast. The lack of coral reefs have been evident  
347 since a massive extinction event, possibly due to cold currents, during the late Miocene (Boekschoten  
348 & Best, 1988). The same extinction event could have also had a similar effect on the tropical brittle  
349 star fauna off this coast. Lastly, phylogenetic diversity turnover between Benguela and the rest of the  
350 east Atlantic provinces was estimated to be high. This province, that contains several old temperate  
351 endemics as well as a few tropical species (Figs. 1d, and S8), is characterised by an upwelling of  
352 colder water (Lutjeharms, 2007) that could limit dispersal of tropical species.

353 Our data contains most of the common tropical brittle star species. Common species frequently  
354 dominate major large-scale patterns (Pos et al., 2014), and we do not expect these patterns of  
355 evolutionary history between RES to substantially alter with increased sampling.

356

358 Our findings based on ancestral range estimations were congruent with other studies showing that the  
359 emergence of barriers heavily structured the biogeography of extant tropical marine taxa (Cowman &  
360 Bellwood, 2013). We found patterns of regional splits within the five families, which were consistent  
361 under both maximum Likelihood and Bayesian approaches (Figs. S9–S14). These splits were also  
362 temporally concordant with the known emergence times of biogeographic barriers in an unconstrained  
363 model (Figs. 2–3). Moreover, a biogeographic model with dispersal constraints in accordance with the  
364 emergence of biogeographic barriers showed strong statistical support (Table S5).

365

366 *Atlantic Opening*

367 We infer that the five families of tropical shallow-water brittle stars included in this study have a  
368 Tethyan origin, as ancestral ranges recovered an IWP or IWP+A distribution for the deeper nodes  
369 (Figs. S10–S14). These reconstructions were consistent with fossil records across the north and west  
370 of the Tethys Sea (Harzhauser et al., 2007; Štorc & Žitt, 2008; Thuy & Kroh, 2011). Tethyan lineages  
371 subsequently regionalised into Atlantic and Indo-West Pacific faunas, as shown by both phylogenetic  
372 diversity metrics and biogeographic reconstructions (Figs. 1 and 3). A similar Tethyan origin has also  
373 been inferred for several other extant tropical marine taxa (staghorn corals, Wallace & Rosen, 2006),  
374 from which sister Indo-West Pacific and Atlantic faunas diverged as a result of the closure of the  
375 Tethys Seaway (TTE: Terminal Tethyan Event, 18–12 Ma; Hou & Li, 2018).

376 In general, A/IWP faunal splits were estimated to have occurred much more frequently during the  
377 Eocene, and less frequently during the late Cretaceous (Ophiidermatidae) and Pliocene (Figs. 2 and  
378 S9a). The older splits in Ophiidermatidae suggested that the opening of the Atlantic Ocean during the  
379 late Cretaceous (110–65 Mya; Perez-Diaz & Eagles, 2017; Hou & Li, 2018) might have affected the  
380 evolution of brittle stars, by acting as an important filter for dispersal, as has been found in fishes  
381 (Floeter et al., 2008).

382 *East Pacific Barrier*

383 The East Pacific Barrier, one of the greatest marine biogeographic barriers for shallow-water species  
384 (Briggs, 1961) can be breached by some taxa (Lessios & Robertson, 2006). We recovered three recent  
385 (Pliocene and Pleistocene) dispersals between the East Pacific and the Indo-West Pacific (Figs. 1–3,  
386 and S10–S14). Although it has been shown that the transport times across the EPB exceeds the larval  
387 life span of most marine taxa, El Niño events could speed up dispersal enough for larvae with longer  
388 life spans (i.e. planktotrophic larvae) to cross this barrier (Wood et al., 2016). *Ophiocoma erinaceus* is  
389 an Indo-West Pacific sexually reproducing species with planktotrophic larvae that has been recorded

390 from the Clipperton Islands, the most western province of the East Pacific. Interestingly, the other two  
391 species with transpacific dispersals (*Ophiocomella sexradia* and *Ophiothela mirabilis*) are fissiparous  
392 (reproducing asexually, but also have sexual reproduction), for which their ability to reproduce  
393 asexually would aid rapid proliferation (Boissin, Egea, Féral & Chenuil, 2015), and successful  
394 colonisation (Mantelatto et al., 2016).

395

#### 396 *Tethyan Seaway*

397 Faunal splits between the Atlantic and Indo-Pacific were estimated with high frequency during the  
398 Eocene (Fig. 2). These divergence events were concordant with the narrowing of the Tethyan Seaway  
399 (50–18 Ma), suggesting it was a driver of divergence events shaping current distributions of tropical  
400 brittle stars (Ophiocomidae, Ophiolepididae, Ophionereididae, and Ophiotrichidae). Although the  
401 splits pre-dated the TTE, our results are congruent with previous findings in other marine taxa  
402 (reviewed in Hou & Li, 2018), for which pre-TTE vicariance has been explained by the emergence of  
403 genetic barriers driven by ecological changes resulting from plate tectonics (Liu, Li, Ugolini,  
404 Momtazi & Hou, 2018). Apparent vicariant events pre-dating the TTE have also been attributed to  
405 calibration errors (Malaquias & Reid, 2009) or selective extinction concealing patterns (Cowman &  
406 Bellwood, 2013). An example of the latter might be the deep (Eocene) split within *Ophionereis*  
407 Lütken, 1859 between the East Atlantic *O. perplexa* (Ziesenhenné, 1940) and an Atlantic clade (Figs.  
408 2, S9, and S13). However, the concordant patterns independently estimated here across five families,  
409 under an unconstrained model (Figs. 2 and 3) and several averaged models (Fig. S9 and Table S5),  
410 suggest a common process driving the evolution of tropical brittle stars.

411 Transitions between the Indo-West Pacific and Atlantic that post-date the TTE can be attributed to  
412 dispersal around South Africa. Dispersals occurring in this region have been documented from fossil  
413 (Vermeji & Rosenberg, 1993) and molecular evidence (Bowen, Muss, Rocha & Grant, 2006), in  
414 which lineages from the Indian Ocean colonised the west Atlantic, with further dispersals into islands  
415 from the Mid-Atlantic Ridge. However, regional transitions inferred from our study did not conform  
416 to this pattern. Species of *Ophiocomella* might have dispersed through South Africa, but the dispersal  
417 route across the three RES was uncertain in our data. Four other dispersals might be inferred around  
418 South Africa, but these represent species (Ophiotrichidae: *Ophiothrix (Ophiothrix) aristulata* Lyman,  
419 1879; Ophiodermatidae: *Ophioderma wahlbergii* Müller & Troschel, 1842, *Cryptopelta aster*  
420 (Lyman, 1879), *Ophiarachnella capensis* (Bell, 1888)) with narrow distribution across the Atlantic  
421 and Indo-West Pacific RES (Table S1). Only the deeper species *O. aristulata* (50–650 m; O'Hara,  
422 1998) has a significant distribution outside southern Africa, being also reported from Australia and  
423 New Zealand (O'Hara, England, Gunasekera & Naughton, 2014), and represents a significant  
424 incursion of an Atlantic clade across the Indian Ocean. However, its pattern of distribution may be

425 more indicative of southern upper bathyal species rather than shallow-water tropical fauna. The other  
426 three species were restricted mostly to South Africa, at the boundaries of both RES. Disjunct  
427 distributional ranges around South Africa have been reported for several taxa, but the site of  
428 disjunction varies (Waters, 2008), consistent with the variable limits of distributional ranges on these  
429 three species of brittle stars. These apparent range expansions could represent warm-adapted taxa that  
430 successfully adapted to more temperate conditions as the tropics contracted, becoming restricted to  
431 South Africa. They could also represent recent (e.g. *O. capensis*) or ancient (e.g. *O. wahlbergii*)  
432 offshoots of a regionalised fauna, but without data on other closely related species it is not possible to  
433 determine the timing and causes of these distributions.

434

#### 435 *Isthmus of Panama*

436 The full emergence of the Isthmus of Panama occurred during the late Pliocene (c. 2.8 Ma), and  
437 caused the divergence of lineages in several marine taxonomic groups (reviewed by Lessios, 2008).  
438 Faunal splits between these two regions also pre-dated the full emergence of the barrier (Figs. 2 and  
439 3), being more frequent during the mid to late Miocene. Geochemical, geochronological and  
440 biological evidence have suggested a complex history of gradual uplift, with deep water seaways  
441 being extinguished during the late Miocene (around 9.2 Ma ago; O'Dea et al., 2016), and reduced  
442 water flow from west to east (Newkirk & Martin, 2009) that might have affected connectivity or  
443 reduced suitable habitat. No separation events were inferred to occur after the complete closure of the  
444 Panamanian Seaway. The only exception to this was the introduced eastern Pacific species *Ophiothela*  
445 *mirabilis* (Mantelatto et al., 2016).

446

#### 447 **Concluding remarks**

448 Phylogenetic diversity and biogeographic historical reconstructions provided evidence of the key role  
449 that tropical biogeographic barriers have played in the diversification of tropical brittle stars. The  
450 extant tropical shallow-water brittle stars were inferred to have a Tethyan origin, from which Atlantic  
451 and Indo-West Pacific faunas diverged. However, these divergence age estimates predate the TTE,  
452 suggesting that changes driven by the narrowing of the Tethyan Seaway shaped spatio-temporal  
453 assemblages more than its final closure. The EPB barrier played an extremely important role in the  
454 evolution of this group, as it has largely prevented colonisation of the East Pacific from the Indo-West  
455 Pacific. Instead, the extant East Pacific fauna diverged from the Atlantic, due to the gradual  
456 emergence of the Isthmus of Panama.

#### 457 **REFERENCES**

- 458 Adams, C.G., Gentry, A.W. & Whybrow, P.J. (1983) Dating the terminal Tethyan event. *Utrecht*  
459 *Micropaleontological Bulletins*, **30**, 273-298.
- 460 Araujo, M.B. & New, M. (2007) Ensemble forecasting of species distributions. *Trends in Ecology and*  
461 *Evolution*, **22**, 42-7.
- 462 Baselga, A. (2010) Partitioning the turnover and nestedness components of beta diversity. *Global*  
463 *Ecology and Biogeography*, **19**, 134-143.
- 464 Baselga, A. & Orme, C.D.L. (2012) betapart: an R package for the study of beta diversity. *Methods in*  
465 *Ecology and Evolution*, **3**, 808-812.
- 466 Boekschoten, G.J. & Best, M.B. (1988) Fossil and recent shallow water corals from the Atlantic  
467 islands off Western Africa *Zoologische Mededelingen*, **62**, 99-112.
- 468 Boissin, E., Egea, E., Féral, J.P. & Chenuil, A. (2015) Contrasting population genetic structures in  
469 Amphipholis squamata, a complex of brooding, self-reproducing sister species sharing life  
470 history traits. *Marine Ecology Progress Series*, **539**, 165-177.
- 471 Bouckaert, R., Heled, J., Kuhnert, D., Vaughan, T., Wu, C.H., Xie, D., . . . Drummond, A.J. (2014) BEAST  
472 2: a software platform for Bayesian evolutionary analysis. *PLoS Comput Biol*, **10**, e1003537.
- 473 Bowen, B.W., Muss, A., Rocha, L.A. & Grant, W.S. (2006) Shallow mtDNA coalescence in Atlantic  
474 pygmy angelfishes (genus *Centropyge*) indicates a recent invasion from the Indian Ocean. *J*  
475 *Hered*, **97**, 1-12.
- 476 Bribiesca-Contreras, G., Verbruggen, H., Hugall, A.F. & O'Hara, T.D. (2017) The importance of  
477 offshore origination revealed through ophiuroid phylogenomics. *Proceedings of the Royal*  
478 *Society B: Biological Sciences*, **284**, 20170160.
- 479 Briggs, J.C. (1961) The East Pacific Barrier and the Distribution of Marine Shore Fishes. *Evolution*, **15**,  
480 545.
- 481 Buerki, S., Forest, F., Alvarez, N., Nylander, J.A.A., Arrigo, N. & Sanmartín, I. (2011) An evaluation of  
482 new parsimony-based versus parametric inference methods in biogeography: a case study  
483 using the globally distributed plant family Sapindaceae. *Journal of Biogeography*, **38**, 531-  
484 550.
- 485 Clarke, E. & Sherrill-Mix, S. (2017) *ggbeeswarm: Categorical Scatter (violin point) plots*.
- 486 Costello, M.J., Tsai, P., Wong, P.S., Cheung, A.K.L., Basher, Z. & Chaudhary, C. (2017) Marine  
487 biogeographic realms and species endemism. *Nature Communications*, **8**, 1057.
- 488 Cowman, P.F. & Bellwood, D.R. (2013) Vicariance across major marine biogeographic barriers:  
489 temporal concordance and the relative intensity of hard versus soft barriers. *Proceedings of*  
490 *the Royal Society B: Biological Sciences*, **280**, 1-8.

491 Cowman, P.F., Parravicini, V., Kulbicki, M. & Floeter, S.R. (2017) The biogeography of tropical reef  
492 fishes: endemism and provinciality through time. *Biological Reviews*, **92**, 2112-2130.

493 Crisp, M.D., Trewick, S.A. & Cook, L.G. (2011) Hypothesis testing in biogeography. *Trends Ecol Evol*,  
494 **26**, 66-72.

495 Faith, D.P. (1992) Conservation evaluation and phylogenetic diversity. *Biological Conservation*, **61**, 1-  
496 10.

497 Floeter, S.R., Rocha, L.A., Robertson, D.R., Joyeux, J.C., Smith-Vaniz, W.F., Wirtz, P., . . . Bernardi, G.  
498 (2008) Atlantic reef fish biogeography and evolution. *Journal of Biogeography*, **35**, 22-47.

499 Greiner, B. & Neugebauer, J. (2013) The rotations opening the Central and Northern Atlantic Ocean:  
500 compilation, drift lines, and flow lines. *International Journal of Earth Sciences*, **102**, 1357-  
501 1376.

502 Grigg, R.W. & Hey, R. (1992) Paleoceanography of the tropical eastern pacific ocean. *Science*, **255**,  
503 172-8.

504 Grueber, C.E., Nakagawa, S., Laws, R.J. & Jamieson, I.G. (2011) Multimodel inference in ecology and  
505 evolution: challenges and solutions. *J Evol Biol*, **24**, 699-711.

506 Harzhauser, M., Kroh, A., Mandic, O., Piller, W.E., Göhlich, U., Reuter, M. & Berning, B. (2007)  
507 Biogeographic responses to geodynamics: A key study all around the Oligo–Miocene Tethyan  
508 Seaway. *Zoologischer Anzeiger - A Journal of Comparative Zoology*, **246**, 241-256.

509 Höhna, S., Landis, M.J., Heath, T.A., Boussau, B., Lartillot, N., Moore, B.R., . . . Ronquist, F. (2016)  
510 RevBayes: Bayesian Phylogenetic Inference Using Graphical Models and an Interactive  
511 Model-Specification Language. *Systematic Biology*, **65**, 726–736.

512 Hou, Z. & Li, S. (2018) Tethyan changes shaped aquatic diversification. *Biological Reviews*, **93**, 874-  
513 896.

514 Hugall, A.F., O'Hara, T.D., Hunjan, S., Nilsen, R. & Moussalli, A. (2016) An Exon-Capture System for  
515 the Entire Class Ophiuroidea. *Molecular Biology and Evolution*, **33**, 281-94.

516 Kamp, P.J.J., Waghorn, D.B. & Nelson, C.S. (1990) Late Eocene–Early Oligocene integrated isotope  
517 stratigraphy and biostratigraphy for paleoshelf sequences in southern Australia:  
518 paleoceanographic implications. *Palaeogeography, Palaeoclimatology, Palaeoecology*, **80**,  
519 311-323.

520 Kass, R., E. & Raftery, A.E. (1995) Bayes Factor. *Journal of the American Statistical Association*, **90**,  
521 773-795.

522 Landis, M.J., Matzke, N.J., Moore, B.R. & Huelsenbeck, J.P. (2013) Bayesian analysis of biogeography  
523 when the number of areas is large. *Syst Biol*, **62**, 789-804.

- 524 Lavor, P., Calvente, A., Versieux, L.M. & Sanmartin, I. (2018) Bayesian spatio-temporal reconstruction  
525 reveals rapid diversification and Pleistocene range expansion in the widespread columnar  
526 cactus *Pilosocereus*. *Journal of Biogeography*, **46**, 238-250.
- 527 Leprieur, F., Albouy, C., De Bortoli, J., Cowman, P.F., Bellwood, D.R. & Mouillot, D. (2012) Quantifying  
528 Phylogenetic Beta Diversity: Distinguishing between 'True' Turnover of Lineages and  
529 Phylogenetic Diversity Gradients. *PLoS ONE*, **7**, e42760.
- 530 Lessios, H.A. (2008) The Great American Schism: Divergence of Marine Organisms After the Rise of  
531 the Central American Isthmus. *Annual Review of Ecology, Evolution, and Systematics*, **39**, 63-  
532 91.
- 533 Lessios, H.A. & Robertson, D.R. (2006) Crossing the impassable: genetic connections in 20 reef fishes  
534 across the eastern Pacific barrier. *Proceedings of the Royal Society B: Biological Sciences*,  
535 **273**, 2201-2208.
- 536 Lessios, H.A., Kessing, B.D. & Pearse, J.S. (2001) Population structure and speciation in tropical seas:  
537 global phylogeography of the sea urchin *Diadema*. *Evolution*, **55**, 955-975.
- 538 Liu, H., Li, S., Ugolini, A., Momtazi, F. & Hou, Z. (2018) Tethyan closure drove tropical marine  
539 biodiversity: Vicariant diversification of intertidal crustaceans. *Journal of Biogeography*, **45**,  
540 941-951.
- 541 Lutjeharms, J.R.E. (2007) Three decades of research on the greater Agulhas Current. *Ocean Science*,  
542 **3**, 129-147.
- 543 Malaquias, M.A.E. & Reid, D.G. (2009) Tethyan vicariance, relictualism and speciation: evidence from  
544 a global molecular phylogeny of the opisthobranch genus *Bulla*. *Journal of Biogeography*, **36**,  
545 1760-1777.
- 546 Mantelatto, M.C., Vidon, L.F., Silveira, R.B., Menegola, C., Rocha, R.M.d. & Creed, J.C. (2016) Host  
547 species of the non-indigenous brittle star *Ophiothela mirabilis* (Echinodermata:  
548 Ophiuroidea): an invasive generalist in Brazil? *Marine Biodiversity Records*, **9**, 1-7.
- 549 Matzke, N.J. (2013) *BioGeoBEARS: BioGeography with Bayesian (and Likelihood) Evolutionary*  
550 *Analysis in R Scripts*. University of California, Berkeley, Berkeley, CA.
- 551 Newkirk, D.R. & Martin, E.E. (2009) Circulation through the Central American Seaway during the  
552 Miocene carbonate crash. *Geology*, **37**, 87-90.
- 553 O'Dea, A., Lessios, H.A., Coates, A.G., Eytan, R.I., Restrepo-Moreno, S.A., Cione, A.L., . . . Jackson, J.B.  
554 (2016) Formation of the Isthmus of Panama. *Sci Adv*, **2**, e1600883.
- 555 O'Hara, T., Hugall, A., Woolley, S., Bribiesca-Contreras, G. & Bax, N. (2019) Contrasting processes  
556 drive ophiuroid phylodiversity across shallow and deep seafloors. *Nature*, **565**, 636-639.

- 557 O'Hara, T.D. (1998) Mortensen's Pacific Expedition: re-identification of ophiuroids (Echinodermata)  
558 from southern Australia. *Streenstrupia*, **24**, 37-50.
- 559 O'Hara, T.D., Rowden, A.A. & Bax, N.J. (2011) A Southern Hemisphere bathyal fauna is distributed in  
560 latitudinal bands. *Current Biology*, **21**, 226-230.
- 561 O'Hara, T.D., England, P.R., Gunasekera, R.M. & Naughton, K.M. (2014) Limited phylogeographic  
562 structure for five bathyal ophiuroids at continental scales. *Deep Sea Research Part I:  
563 Oceanographic Research Papers*, **84**, 18-28.
- 564 O'Hara, T.D., Hugall, A.F., Thuy, B., Stöhr, S. & Martynov, A.V. (2017) Restructuring higher taxonomy  
565 using broad-scale phylogenomics: The living Ophiuroidea. *Molecular Phylogenetics and  
566 Evolution*, **107**, 415-430.
- 567 O'Hara, T.D., Hugall, A.F., Cisternas, P.A., Boissin, E., Bribiesca-Contreras, G., Sellanes, J., . . . Byrne,  
568 M. (2018) Phylogenomics, life history and morphological evolution of ophiocomid  
569 brittlestars. *Mol Phylogenet Evol*, **130**, 67-80.
- 570 Paradis, E., Claude, J. & Strimmer, K. (2004) APE: Analyses of Phylogenetics and Evolution in R  
571 language. *Bioinformatics*, **20**, 289-290.
- 572 Perez-Diaz, L. & Eagles, G. (2017) South Atlantic paleobathymetry since early Cretaceous. *Sci Rep*, **7**,  
573 11819.
- 574 Pos, E., Guevara Andino, J.E., Sabatier, D., Molino, J.F., Pitman, N., Mogollon, H., . . . Ter Steege, H.  
575 (2014) Are all species necessary to reveal ecologically important patterns? *Ecology and  
576 Evolution*, **4**, 4626-4636.
- 577 R Core Team (2017) *R: A language and environment for statistical computing*. R Foundation for  
578 *Statistical Computing*. R Foundation for Statistical Computing.
- 579 Ree, R.H. & Smith, S.A. (2008) Maximum likelihood inference of geographic range evolution by  
580 dispersal, local extinction, and cladogenesis. *Syst Biol*, **57**, 4-14.
- 581 Ree, R.H. & Sanmartín, I. (2009) Prospects and challenges for parametric models in historical  
582 biogeographical inference. *Journal of Biogeography*, **36**, 1211-1220.
- 583 Ree, R.H. & Sanmartín, I. (2018) Conceptual and statistical problems with the DEC+J model of  
584 founder-event speciation and its comparison with DEC via model selection. *Journal of  
585 Biogeography*, **45**, 741-749.
- 586 Ree, R.H., Moore, B.R., Webb, C.O. & Donoghue, M.J. (2005) A likelihood framework for inferring the  
587 evolution of geographic range on phylogenetic trees. *Evolution*, **59**, 2299-2311.
- 588 Ronquist, F. (1997) Dispersal-Vicariance Analysis: a new approach to the quantification of historical  
589 biogeography. *Systematic Biology*, **46**, 195-203.

- 590 Sanmartín, I. (2007) Event-based biogeography: integrating patterns, processes, and time.  
591 *Biogeography in a changing world* (ed. by M.C. Ebach and R.S. Tangney), pp. 135-156. Taylor  
592 & Francis, London.
- 593 Spalding, M.D., Fox, H.E., Allen, G.R., Davidson, N., Ferdana, Z.A., Finlayson, M., . . . Robertson, J.  
594 (2007) Marine ecoregions of the world: a bioregionalization of coastal and shelf areas.  
595 *BioScience*, **57**, 573-583.
- 596 Stöhr, S., O'Hara, T.D. & Thuy, B. (2012) Global diversity of brittle stars (Echinodermata:  
597 Ophiuroidea). *PLoS One*, **7**, e31940.
- 598 Štorc, R. & Žitň, J. (2008) Late Turonian ophiuroids (Echinodermata) from the Bohemian Cretaceous  
599 Basin, Czech Republic. *Bulletin of Geosciences*, 123-140.
- 600 Thode, V.A., Sanmartin, I. & Lohmann, L.G. (2019) Contrasting patterns of diversification between  
601 Amazonian and Atlantic forest clades of Neotropical lianas (Amphilophium, Bignoniaceae)  
602 inferred from plastid genomic data. *Molecular Phylogenetics and Evolution*, **133**, 92-106.
- 603 Thuy, B. & Kroh, A. (2011) Barremian ophiuroids from the Serre de Bleyton (Drôme, SE France).  
604 *Annalen des Naturhistorischen Museums in Wien, Serie A*, **113**, 777–807.
- 605 Vermeji, G.J. & Rosenberg, G. (1993) Giving and receiving: the tropical Atlantic as donor and  
606 recipient region for invading species. *American Malacological Bulletin*, **10**, 181-194.
- 607 Wallace, C.C. & Rosen, B.R. (2006) Diverse staghorn corals (*Acropora*) in high-latitude Eocene  
608 assemblages: implications for the evolution of modern diversity patterns of reef corals.  
609 *Proceedings of the Royal Society B: Biological Sciences*, **273**, 975-982.
- 610 Waters, J.M. (2008) Driven by the West Wind Drift? A synthesis of southern temperate marine  
611 biogeography, with new directions for dispersalism. *Journal of Biogeography*, **35**, 417-427.
- 612 Wood, S., Baums, I.B., Paris, C.B., Ridgwell, A., Kessler, W.S. & Hendy, E.J. (2016) El Niño and coral  
613 larval dispersal across the eastern Pacific marine barrier. *Nat Commun*, **7**, 12571.
- 614 Woolley, S.N., Tittensor, D.P., Dunstan, P.K., Guillera-Arroita, G., Lahoz-Monfort, J.J., Wintle, B.A., . . .  
615 O'Hara, T.D. (2016) Deep-sea diversity patterns are shaped by energy availability. *Nature*,  
616 **533**, 393-396.

617

#### 618 **Code and data availability**

619 See supplementary.

#### 620 **Conflict of interest**

621 All authors declare no conflict of interest.

622

623 **Biosketch**

624 The list of authors includes echinoderm researchers with experience in taxonomy, phylogenetics and  
625 biogeography.

626

627 **Author contributions**

628 G.B.C., H.V. A.H. and T.O.H. conceived the study. T.O.H. and A.H. contributed data. G.B.C.  
629 performed analyses and drafted the manuscript. All authors contributed to the final manuscript.

630

631 **Supplementary information**

632 Table S1. Absence/presence of species of brittle stars by biogeographic provinces.

633 Table S2. Pairwise comparisons of phylogenetic beta diversity of brittle stars between biogeographic  
634 provinces based on the phylogenetic Sørensen ( $pSor$ ) dissimilarity index, and decomposition into  
635 turnover ( $pSor_{turn}$ ) and nestedness ( $pSor_{ne}$ ).

636 Figure S1. Time-calibrated phylogeny of the class Ophiuroidea.

637 Figure S1. Sampled-species richness of brittle stars by biogeographic province. Figure S2. Time-  
638 calibrated tree of the family Ophiocomidae. Figure S3. Time-calibrated tree of the family  
639 Ophiodermatidae.

640 Figure S4. Time-calibrated tree of the family Ophiolepididae.

641 Figure S5. Time-calibrated tree of the family Ophionereididae.

642 Figure S6. Time-calibrated tree of the family Ophiotrichidae.

643 Figure S7. Turnover component from brittle star beta diversity index of biogeographic provinces.

644 Table S3. Within-RES statistics for brittle star phylogenetic turnover estimates between provinces.

645 Table S4. Ln-Bayes factors for biogeographic model selection for each brittle star family.

646 Table S5. Different models considered for the biogeographic history of tropical shallow brittle stars.

647 Figure S8. Integrated posterior temporal distribution of brittle star faunal splits.

648 Figure S9. Biogeographic history of the family Ophiocomidae.

- 649 Figure S10. Biogeographic history of the family Ophiidermatidae.
- 650 Figure S11. Biogeographic history of the family Ophiolepididae.
- 651 Figure S12. Biogeographic history of the family Ophionereididae.
- 652 Figure S13. Biogeographic history of the family Ophiotrichidae.
- 653 Supplementary File 1. BEAST xml file for the family Ophiocomidae.
- 654 Supplementary File 2. BEAST xml file for the family Ophiidermatidae.
- 655 Supplementary File 3. BEAST xml file for the family Ophiolepididae.
- 656 Supplementary File 4. BEAST xml file for the family Ophionereididae.
- 657 Supplementary File 5. BEAST xml file for the family Ophiotrichidae.
- 658 Supplementary File 6. Combined log files from two BEAST runs for the family Ophiocomidae.
- 659 Supplementary File 7. Combined log files from two BEAST runs for the family Ophiidermatidae.
- 660 Supplementary File 8. Combined log files from two BEAST runs for the family Ophiolepididae.
- 661 Supplementary File 9. Combined log files from two BEAST runs for the family Ophionereididae.
- 662 Supplementary File 10. Combined log files from two BEAST runs for the family Ophiotrichidae.
- 663 Supplementary File 11. Sample of 100 BEAST posterior sample trees from two combined runs for the  
664 family Ophiocomidae.
- 665 Supplementary File 12. Sample of 100 BEAST posterior sample trees from two combined runs for the  
666 family Ophiidermatidae.
- 667 Supplementary File 13. Sample of 100 BEAST posterior sample trees from two combined runs for the  
668 family Ophiolepididae.
- 669 Supplementary File 14. Sample of 100 BEAST posterior sample trees from two combined runs for the  
670 family Ophionereididae.
- 671 Supplementary File 15. Sample of 100 BEAST posterior sample trees from two combined runs for the  
672 family Ophiotrichidae.
- 673 Supplementary File 16. R scripts.
- 674 Supplementary File 17. REVBAYES scripts.

675

676

677

678 **Table 1. Number of described species of brittle stars according to O’Hara et al (2017) per family, tropical**  
 679 **shallow-water species and species contained in the phylogenies.**

FAMILY	NUMBER OF DESCRIBED SPECIES	NUMBER OF KNOWN TROPICAL SPECIES	TROPICAL SPECIES WITH SEQUENCES	NUMBER OF MONOPHYLETIC CLADES AND SPECIES PRUNED
Ophiocomidae	45	43 (96%)	41 (95%)	0+ 1 spp
Ophiodermatidae	57	41 (72%)	28 (68%)	1(2 spp) + 6 spp
Ophionereididae	56	49 (88%)	27 (55%)	3 (2, 2, and 6 spp) + 5 spp*
Ophiolepididae	38	20 (53%)	17 (85%)	2 (4 and 4 spp)
Ophiotrichidae	170	135 (79%)	60 (36%)	1(4 spp) + 1 spp*

680 \* Two additional tips were removed as they represent cryptic species of known species that are already  
 681 included.

682 Details of the number of described species, species inhabiting tropical shallow-water habitats, species with  
 683 genetic data available and number of monophyletic clades and species pruned from family-level phylogenies are  
 684 shown. Additionally, percentage of tropical species, as well as percentage of tropical taxa sampled per family is  
 685 shown in brackets. Pruned species represent deep-sea taxa, non-tropical or duplicates of tropical shelf taxa  
 686 (details in Figs. S3–S7).

687

688

689 **Table 2. Metrics of phylogenetic beta diversity of brittle star assemblages, and corresponding turnover**  
 690 **and nestedness fractions for delimited regions of evolutionary significance (RES).**

	REGIONS OF EVOLUTIONARY SIGNIFICANCE	pSor	pSor <sub>turn</sub>	pSor <sub>ne</sub>
<b>Observed</b>	Atlantic/East Pacific	0.529	0.359	0.169
	East Pacific/Indo-West Pacific	0.854	0.629	0.225

	Atlantic/Indo-West Pacific	0.779	0.675	0.104
<b>Standardised</b>	Atlantic/East Pacific	-1.751	-2.655	3.072
<b>Effect Size (SES)*</b>	East Pacific/Indo-West Pacific	5.795	5.166	-2.283
	Atlantic/Indo-West Pacific	6.403	7.264	-4.449

691 \*SES values  $\geq 1.96$  and  $\leq -1.96$  indicated a PBD higher and lower, respectively, than expected from taxonomic  
692 assemblages. pSor, phylogenetic Sørensen index; pSor<sub>turn</sub>, phylogenetic turnover; pSor<sub>ne</sub>, phylogenetic  
693 nestedness.

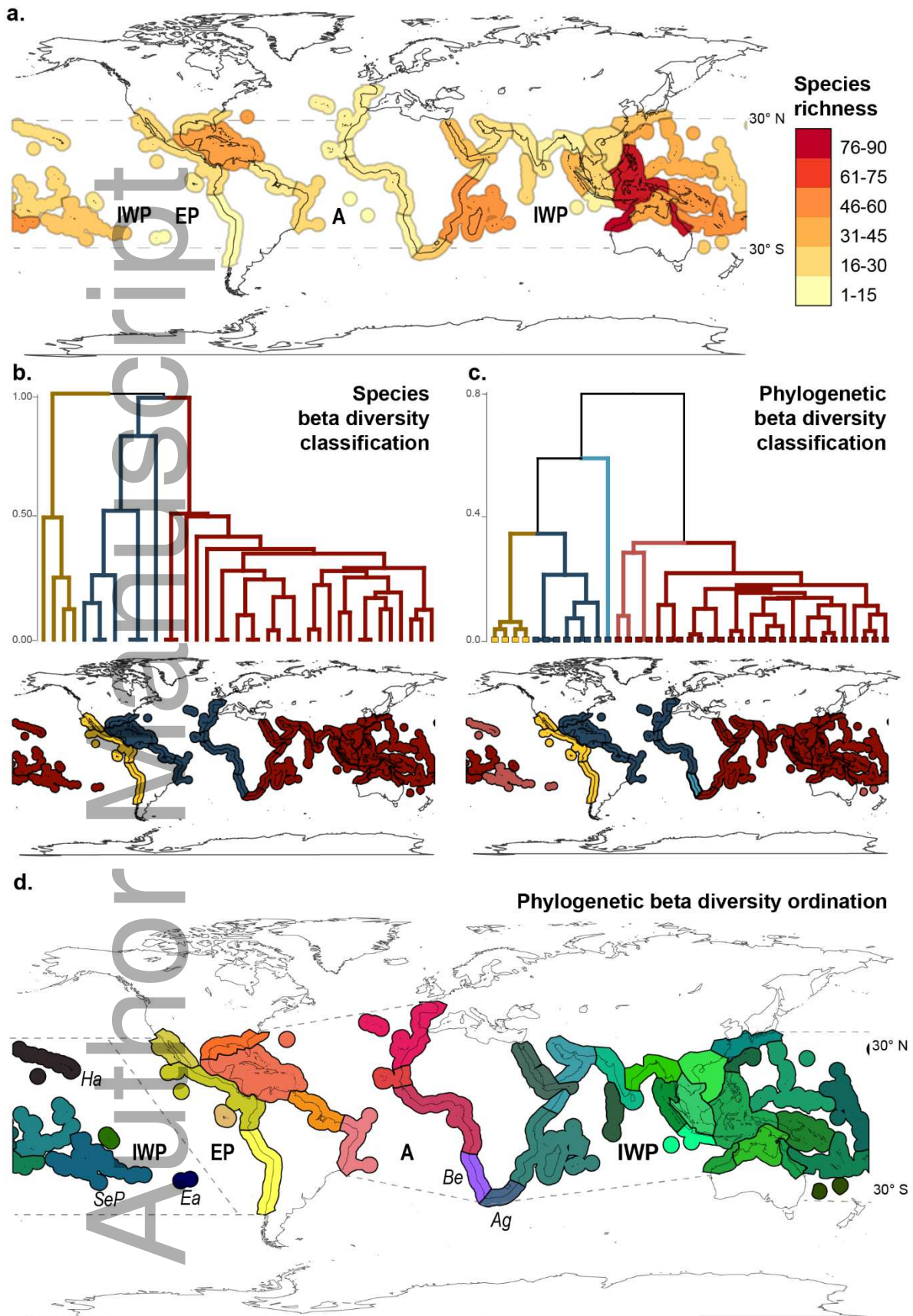
694

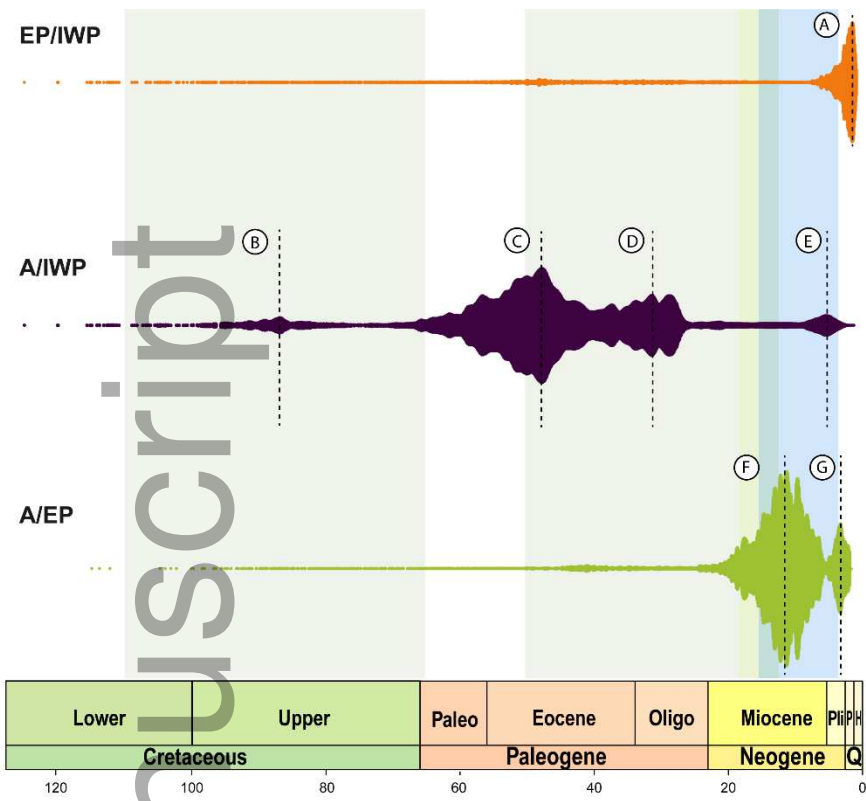
695 **Table 3. Summary of numbers of nodes associated with brittle star faunal splits between Atlantic, Indo-**  
696 **West Pacific and East Pacific oceans.**

FAMILY	A/EP		A/IWP			EP/IWP
	ALL	IoP	ALL	AO	NTS	ALL
Ophiocomidae	2	2	5	0	4	2
Ophiodermatidae	5	5	2	2	0	0
Ophiolepididae	2	2	2	0	1	0
Ophionereididae	3	1	1	0	1	1
Ophiotrichidae	2	2	2	0	1	1
<b>TOTAL</b>	<b>14</b>	<b>12</b>	<b>12</b>	<b>2</b>	<b>7</b>	<b>4</b>

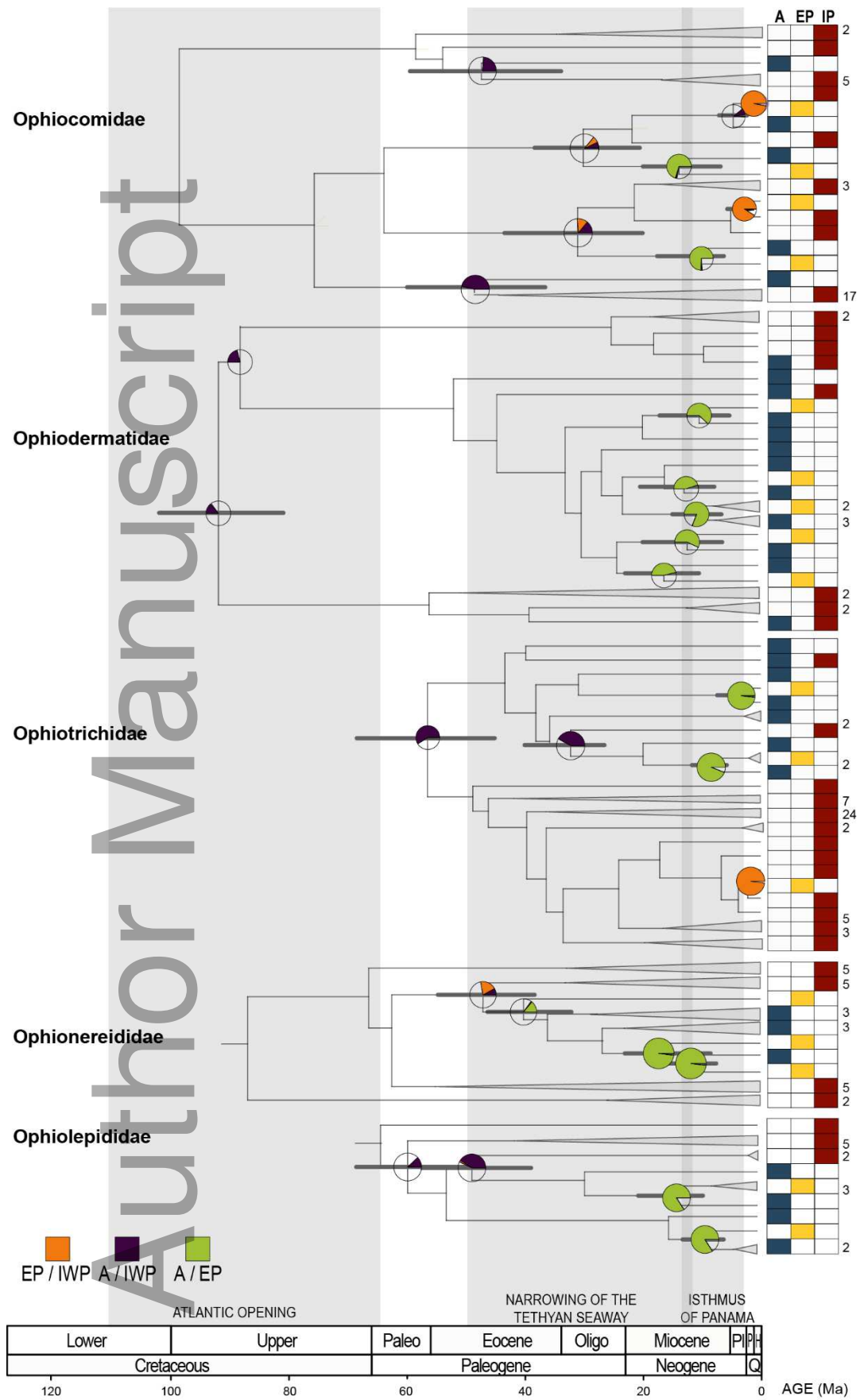
697 Columns include the number of nodes for which brittle star faunal splits were recovered with at least 10%  
698 frequency and temporally consistent with biogeographic events. Atlantic Opening (AO), narrowing of the  
699 Tethyan Seaway (NTS), rise of the Isthmus of Panama (IoP), Atlantic (A), East Pacific (EP), and Indo-West  
700 Pacific (IWP).

701





703



704

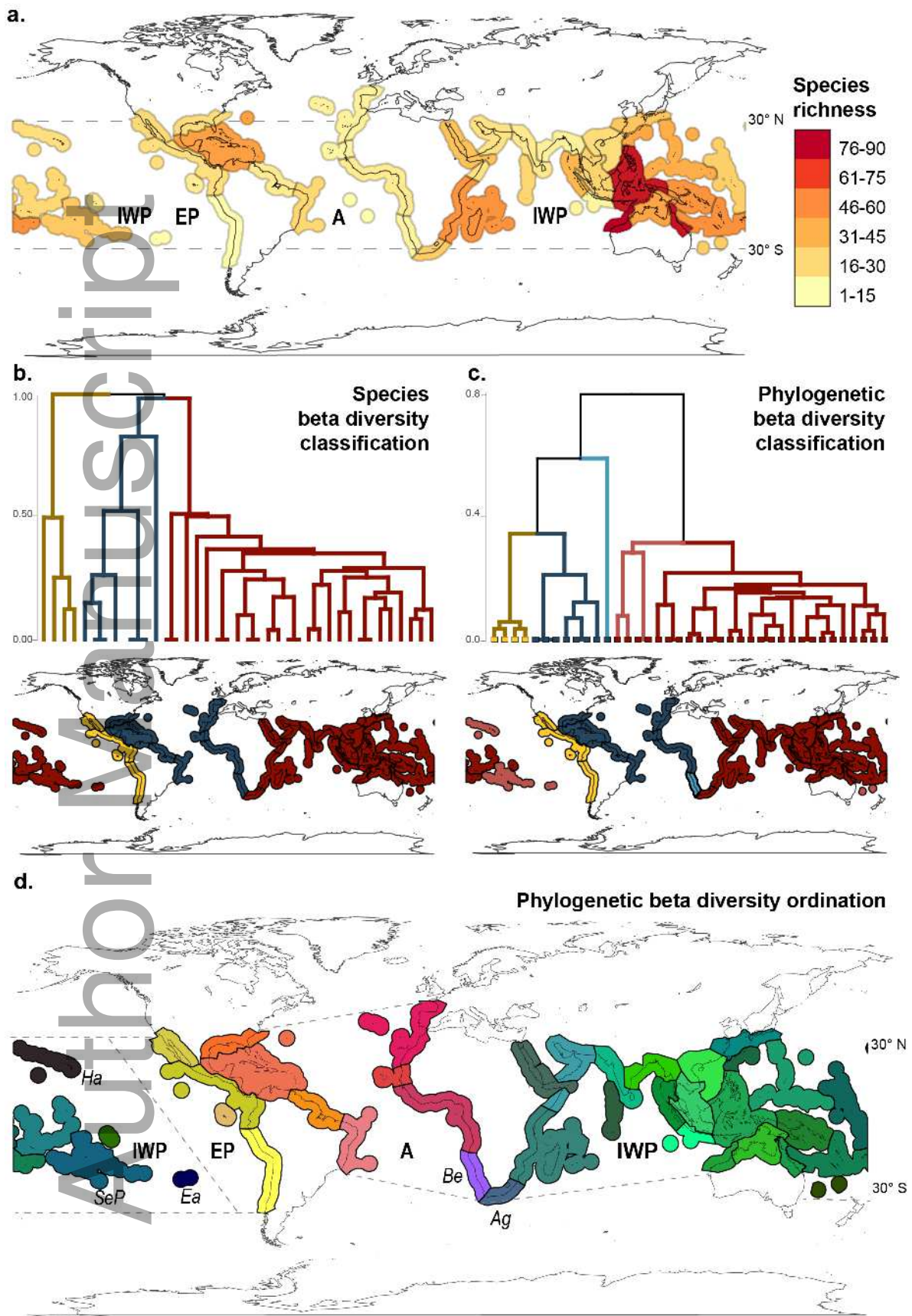
705

706 **Figure legends**

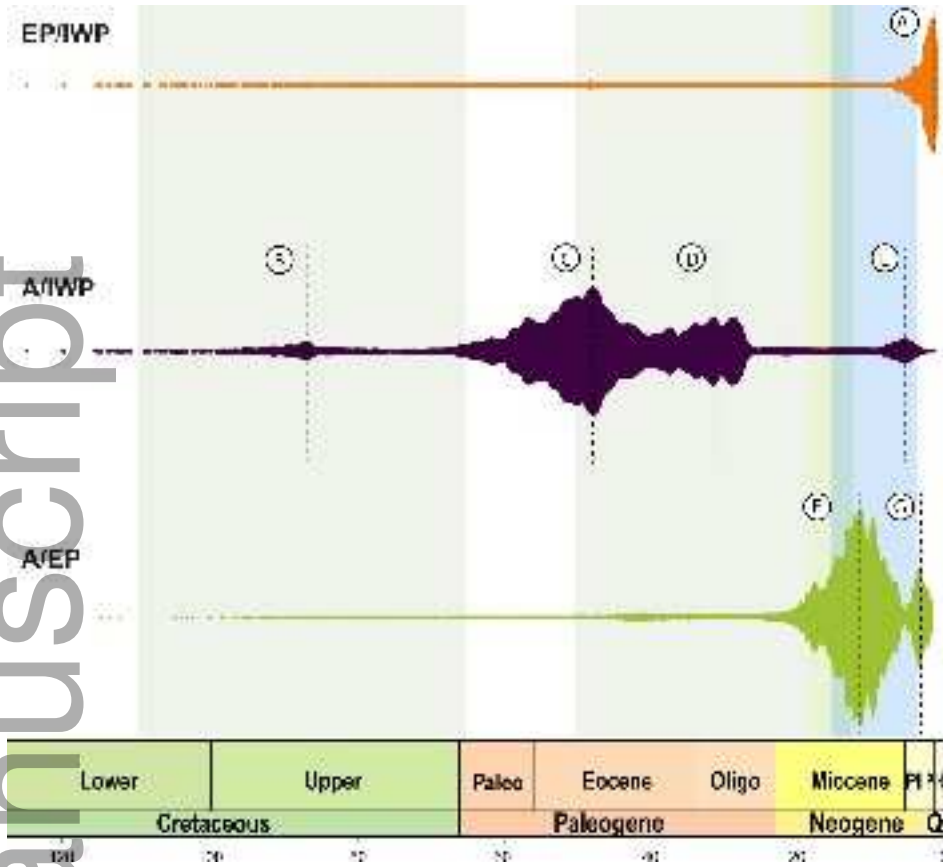
707 **Figure 1. Distribution of beta diversity of five families of tropical shelf brittle stars** | (a) Species  
708 richness by tropical/temperate MEOW provinces (Spalding et al., 2007). Provinces clustered, using  
709 UPGMA, as potential regions of evolutionary significance (RES) using metrics of species turnover  
710 ( $S_{\text{turn}}$ , b) and phylogenetic turnover ( $pS_{\text{turn}}$ , c) are shown in yellow (EP), blue (A) and red (IWP).  
711 Two smaller clusters, recovered by phylogenetic turnover, have branches shown in pink and light  
712 blue, while leaves in dendrogram show our three chosen RES. (d) RGB representation of the three  
713 axes of a NMDS ordination of phylogenetic turnover between provinces, with similar colours  
714 indicating regions that are phylogenetically similar. IWP, Indo-West Pacific; EP, East Pacific; A,  
715 Atlantic; Ha, Hawaii; SeP, Southeast Polynesia; Ea, Easter Island; Be, Benguela; Ag, Agulhas (for  
716 other province names, see Spalding et al., 2007).

717 **Figure 2. Integrated posterior temporal distribution of brittle star faunal splits.** | Posterior  
718 density of faunal splits recovered for all nodes, under a simple DEC model, on 100 posterior sample  
719 trees for each of the five families of brittle stars. Width (y axis) of the violin plots is proportional to  
720 the number of data points. Peaks on the frequency of faunal splits between EP/IWP (A), A/IWP (B–E)  
721 and A/EP (F) are indicated. A, Atlantic; IWP, Indo-West Pacific; EP, East Pacific. Time associated  
722 with the emergence of specific barriers is indicated with coloured bands, from left to right: Atlantic  
723 Opening, narrowing of the Tethyan Seaway, Terminal Tethyan Event, and rise of the Isthmus of  
724 Panama.

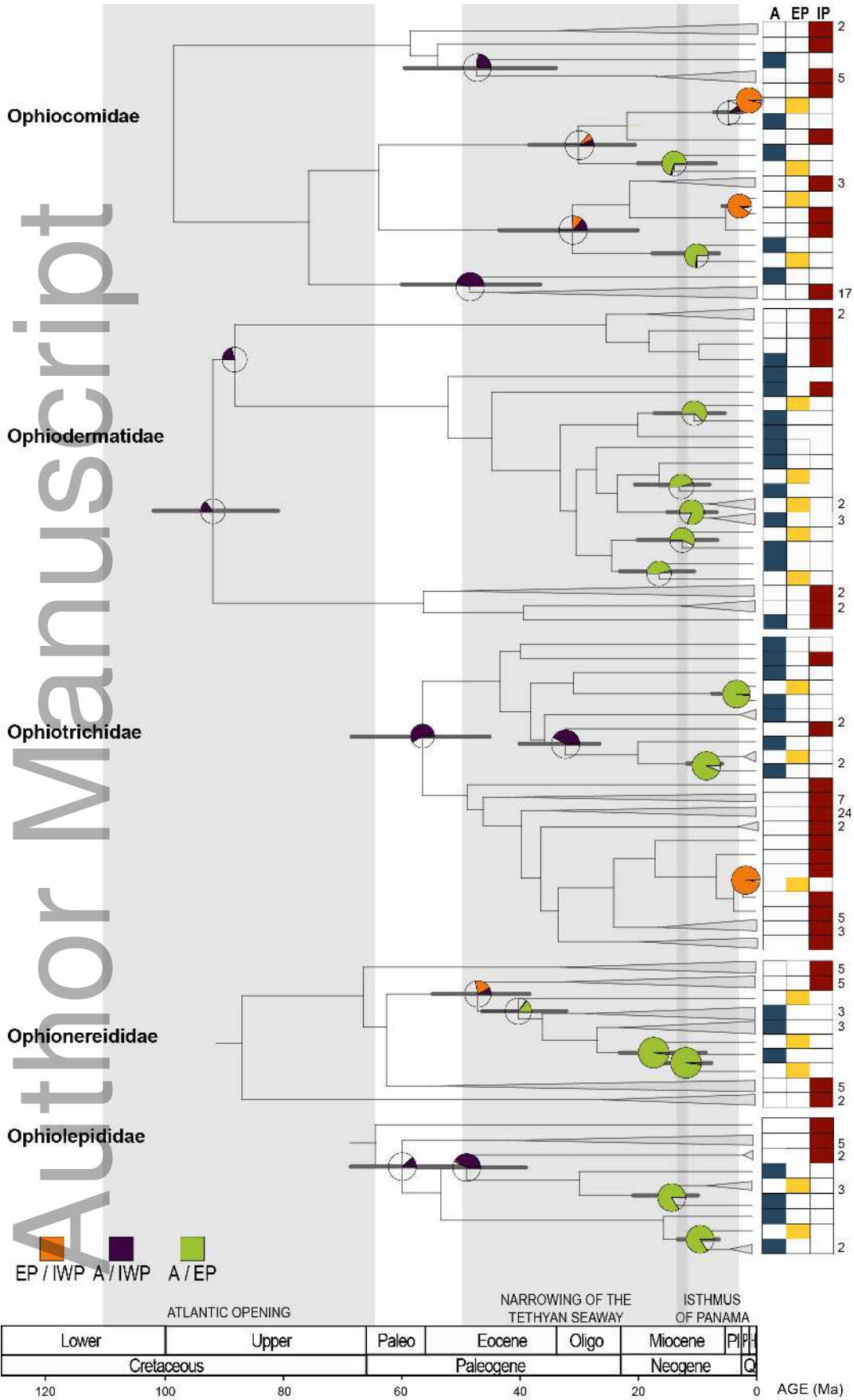
725 **Figure 3. Inferred biogeographic histories of five families of tropical shelf brittle stars.** | Faunal  
726 splits (A/IWP, EP/IWP, A/EP), as estimated from a simple DEC model and averaged across 1-100  
727 posterior sample trees, mapped onto family-level BEAST consensus trees. Only nodes for which  
728 faunal splits were recovered with at least 10% frequency are annotated with age 95%CI bars and  
729 transition frequency pie-charts. Node pie-charts are coloured according to each of the three faunal  
730 splits, with no colour indicating other events at cladogenesis (e.g. sympatry). Species distributions are  
731 shown for each of the three regions: Atlantic (A), East Pacific (EP) and Indo-West Pacific (IWP).  
732 Clades endemic to a region are collapsed, not to scale, but the number of species in each is indicated  
733 on the right.



jbi\_13620\_f1.tif



jbi\_13620\_f2.tif



jbi\_13620\_f3.tif